I&EC research
Industrial & Engineering Chemistry Research

Article

pubs.acs.org/IECR

Multichannel Tubular Ceramic Membrane for Water and Heat Recovery from Waste Gas Streams

Maowen Yue,[†] Shuaifei Zhao,*[,†,‡] Paul H. M. Feron,[§] and Hong Qi*[,†]

[†]State Key Laboratory of Material-Oriented Chemical Engineering, Membrane Science and Technology Research Center, Nanjing Tech University, Nanjing 210009, Jiangsu, China

[‡]Faculty of Science & Engineering, Macquarie University, North Ryde, New South Wales 2109, Australia

[§]CSIRO Energy, P.O. Box 330, Newcastle, New South Wales 2300, Australia

ABSTRACT: For the first time, we report a multichannel ceramic tubular membrane for water and heat recovery from gas streams. Mass and heat transfer performances of the multichannel tubular membrane are systematically investigated and compared with those of a monochannel tubular membrane. Compared with the monochannel tubular membrane, the multichannel membrane has much larger mass and heat transfer resistances, leading to lower mass and heat transfer rates. Operational parameters (e.g., fluid velocities and transmembrane pressure difference) have insignificant effects on mass and heat transfer in the multichannel membrane, suggesting that transfer resistance from the membrane itself rather than the boundary layers dominates mass and heat transfer in membrane condensation. The multichannel membrane shows larger volumetric mass and heat transfer coefficients, comparable water recoveries, but lower heat recoveries compared with the monochannel tubular membrane. Water and heat recoveries exhibit a proportional correlation using the multichannel tubular membrane, indicating that heat transport is governed by convective heat transfer, and thermal conductive heat transfer is negligible in the multichannel membrane.

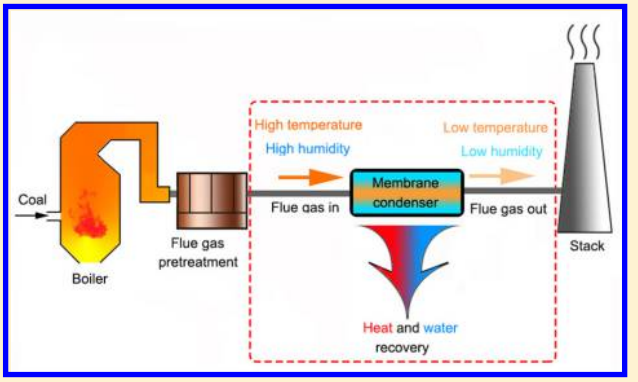

1. INTRODUCTION

Demands for safe water and accessible energy are continuously growing due to worldwide population growth and economic development with rapid industrialization and urbanization.[1,2] Waste gaseous streams from industrial processes, such as power generation and dry operations, contain large quantities of water vapor and thus represent large losses of latent heat. They can be considered to be a valuable alternative source of water and process heat if cost-effective recovery approaches can be developed.[3]

In the past decade, various membrane processes have been used for water and/or heat recovery from gaseous streams (e.g., flue gas).[4−11] These membrane processes are mainly based on water vapor condensation on the feed side using hydrophobic porous membranes[6,7,9] or on the permeate side using hydrophilic nanoporous membranes.[4,10,11] Water recovery in the range 20−60% and 30−80% heat recovery from flue gas between 50 and 90 °C are achievable.[4,6,10] Such performances can significantly improve the thermal efficiency of the boiler[11] and make the power plant self-sufficient in terms of water.[3]

The Gas Technology Institute (GTI) in the United States has demonstrated a membrane condensation technology, called the "transport membrane condenser", for water and heat recovery from coal-fired plant flue gas.[4,11,12] The technology is based on a nanoporous ceramic tubular membrane with a selective layer (pore size 6−8 nm), an intermediate layer (pore size 50 nm), and a substrate (pore size 400 nm).[4] The recovered water and heat can be directly used as makeup water for a power plant boiler, achieving significant water and energy savings.

Previously, we employed a monochannel tubular ceramic membrane as the condenser to recover water and heat from water vapor saturated gas streams, and achieved reasonably high water and heat recoveries.[10] Nevertheless, monochannel ceramic tubes have relatively small cross-sectional (i.e., contact) areas and are fragile in extended length. These disadvantages of monochannel tubes restrict their large-scale industrial applications. Two strategies can be adopted to overcome these disadvantages: one is to use bundled monochannel ceramic tubes (Figure 1A) and the other is to employ multichannel ceramic tubes (Figure 1B).

Bundled monochannel tubes have been employed by GTI to recover water and heat from coal-fired power plant flue gas.[4] Until now, however, few studies based on multichannel ceramic tubes have been reported. Multichannel ceramic tubes are also known as multichannel ceramic monoliths or ceramic honeycombs.[13] They have been widely used in various industrial

Received: January 18, 2016
Revised: February 19, 2016
Accepted: February 22, 2016

DOI: 10.1021/acs.iecr.6b00242
Ind. Eng. Chem. Res. XXXX, XXX, XXX−XXX

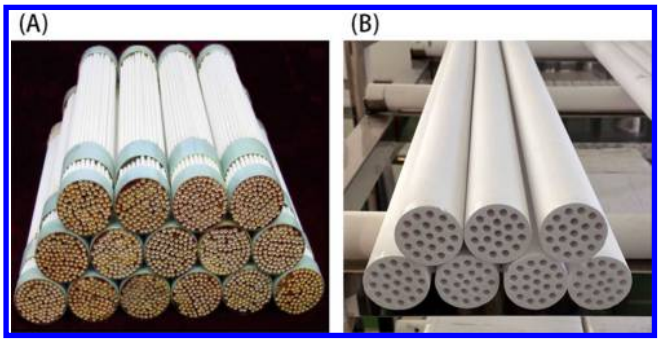

Figure 1. Bundled monochannel ceramic tubes (A) and multichannel ceramic tubes (B).

processes such as catalytic reactions and membrane filtration due to their large cross-sectional areas and excellent mechanical strength.[14]

In this study, we employ a 19-channel ceramic tube (Figure 1B) as the membrane condenser to recover water and heat from gas streams containing high water vapor content. Effects of operational parameters, including gas velocity, water velocity, transmembrane pressure difference, and inlet gas temperature on mass and heat transfer in the multichannel membrane are investigated and compared with our previous results using a monochannel membrane.

2. HEAT AND MASS TRANSFER IN MEMBRANE CONDENSATION

2.1. Heat Transfer. Heat transfer in a membrane condenser can be described by the resistance-in-series model, including resistances from the bulk gas, gas boundary layer, condensate film, membrane, liquid boundary layer, and bulk liquid (Figure 2). Heat transfer mainly occurs via four consecutive steps: (i) convective heat transfer across the gas boundary layer from the bulk gas to the condensate film on the membrane surface, (ii) conductive heat transfer from the condensate film to the membrane surface, (iii) conductive and convective heat transport across the nanoporous membrane, and (iv) convective heat flow across the liquid boundary layer to the bulk liquid.[15,16] The membrane condenser can be regarded as a special heat exchanger in which both mass and heat transfer may occur.[17−19] The overall heat transfer coefficient (U) can be obtained by

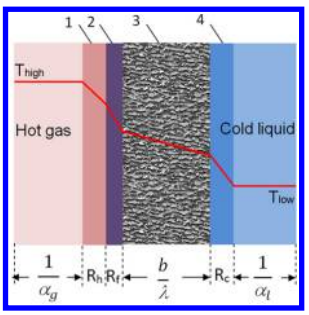

Figure 2. Heat transfer from a hot gas to a cold liquid across a membrane with water vapor condensation. 1, Gas boundary layer; 2, condensate film; 3, membrane; 4, cold liquid boundary layer. α_g and α_l are the heat transfer coefficients in the bulk gas and liquid, respectively; R_h, R_c, and R_f are the heat transfer resistances in the hot side boundary layer, cold side boundary layer, and condensate film, respectively; b is the membrane thickness; λ is the heat transfer coefficient of the membrane.

$$Q = UA\Delta t_m \tag{1}$$

where Q is the heat transfer rate (W), A is the effective contact area (m^2), and Δt_m is the log mean temperature difference (K) between the hot stream and the cold stream in the membrane heat exchanger.

When using a cylindrical structure such as a monochannel ceramic tube as the membrane condenser, the conductive heat transfer resistance can be described as[11]

$$R = \frac{1}{2\pi L} \ln \frac{d_o}{d_i} \tag{2}$$

where λ is the thermal conductivity of tube ($W{\cdot}m^{-1}K^{-1}$), L is the tube length (m), and d_o and d_i are the outer and inner diameters of the tube (m), respectively. For a porous ceramic membrane wetted by water, the thermal conductivity of the membrane (λ_m) is given by

$$\lambda_m = (1-\gamma)\lambda_{ceramic} + \gamma\lambda_{water} \tag{3}$$

where $\lambda_{ceramic}$ and λ_{water} are the thermal conductivities of the ceramic material and water respectively; γ is the membrane porosity.

2.2. Mass Transfer. According to the Kelvin equation, the occurrence of capillary condensation is mainly dependent on the relative pressure (the ratio of the equilibrium pressure to the saturation vapor pressure).[20] In nanoporous structures with pores between 2 and 50 nm, van de Waals force causes water vapor to undergo multilayer adsorption in the membrane capillaries (pores) until the pores fill with liquid.[21,22] When the pore-filling pressure (i.e., capillary condensation pressure) approaches the water vapor saturation pressure, capillary condensation begins to occur. The Kelvin equation has been used to predict capillary condensation pressure[20]

$$\frac{\rho RT}{M} \ln \frac{P_t}{P_0} = -2\frac{\cos\theta}{r} \tag{4}$$

where ρ is the water density ($kg{\cdot}m^{-3}$), R is the molar gas constant ($J{\cdot}mol^{-1}{\cdot}K^{-1}$), T is the water absolute temperature (K), M is the molar weight of water ($kg{\cdot}mol^{-1}$), P_t is the equilibrium pressure (Pa), P_0 is the saturation pressure (Pa), θ is the contact angle (deg), and r is the radius of the cylindrical capillary (m).

Six flow modes were employed to describe mass transfer in the process.[20,22] In the extreme case, when the entire pore is filled with bulk condensate, the condensate flow obeys the Hagen−Poiseuille equation:

$$J_c = \frac{\varepsilon}{\tau}\frac{\rho\pi r^4}{8M\mu} \tag{5}$$

where ε is the membrane porosity, τ is the membrane tortuosity, and μ is the condensate viscosity (Pa·s).

In reality, however, mass transfer in the nanopore is much more complicated due to the noncylindrical structure of the membrane pore and the effects of pore size distribution.[23]

3. MATERIALS AND METHODS

3.1. Multichannel Tubular Ceramic Membrane. A 19-channel tubular ceramic membrane (Figure 1B) was supplied by Jiangsu Jiuwu High-Tech Co., Ltd. (a spinoff from Nanjing Tech University), employing the ceramic support developed in

DOI: 10.1021/acs.iecr.6b00242
Ind. Eng. Chem. Res. XXXX, XXX, XXX−XXX

our group.[24] The membrane selective layer is coated on the inner side of each channel. The physical parameters of the multichannel ceramic membrane are summarized in Table 1.

Table 1. Physical Characteristics of the Multichannel Ceramic Membrane

membrane parameter	value
total length	0.5 m
effective length	0.46 m
membrane outer diameter	0.031 m
channel inner diameter	0.0038 m
channel number	19
membrane mean pore size	$\sim 1 \times 10^{-8}$ m
effective membrane area	0.1043 m^2

The multichannel ceramic membrane has pore size distributions (nominal pore size 8−10 nm) and body porosity (30−35%) very similar to those of the monochannel membrane used in our previous work,[10] due to the same material and the same fabrication conditions. According to the three-point bending measurement, the mechanical strengths of the multichannel and the monochannel ceramic membranes are 5000−6000 and 200−300 MPa, respectively.

3.2. Experimental Setup. The experimental setup mainly consists of a steam generator, a membrane module, and a cooling system for water and heat collection (Figure 3). Air was pumped into the steam generator, and the air flow rate was monitored by a gas flow meter. Humidified gas then went to the tube side of a multichannel ceramic membrane. A humidity transmitter (Vaisala, Finland) and a thermocouple were used to measure the inlet gas stream humidity and temperature, respectively. The stainless tubing of the gas stream was thermally insulated and heated to the required temperatures by heating belts with a temperature controller. The measured humidity of the gas stream was in the range 97−100% (i.e., approaching saturated). Cold water was countercurrently circulated on the shell side of the ceramic tube.

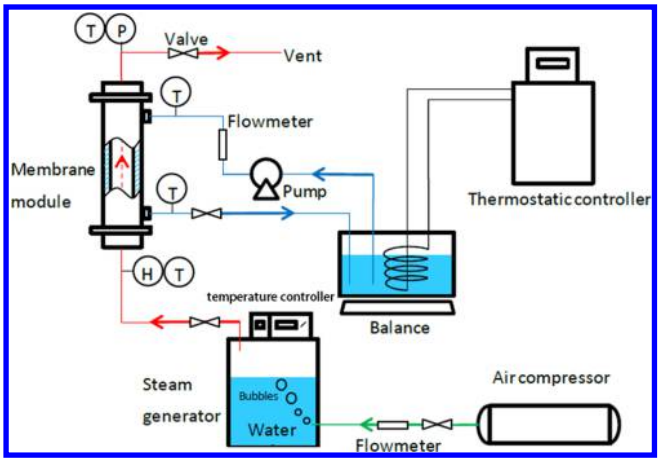

Figure 3. Schematic diagram of the experimental setup for water and heat recovery. H = humidity transmitter; T = thermocouple.

In each experimental run, the coolant water inlet temperature was maintained stable with a thermostatic controller. Flow rates and inlet and outlet temperatures of the coolant water were measured for heat transfer determination. Weight change of the water was monitored with a balance for mass transfer determination. Data recording was started once the mass transfer and heat transfer became relatively stable (i.e., mass and heat transports became balanced when there was no change in temperature and humidity for the inlet and outlet gas). Time for mass and heat balancing varied (from 1 to 2 h) with the experimental conditions. For each experimental run, weight and temperature data were recorded for at least 30 min at a time interval of 5 min after mass and heat transfer became relatively stable. Uncertainties in the measurements were gas side temperature ±2.5%, liquid side temperature ±6.1%, gas flow rate ±6.2%, and liquid flow rate ±4%. Mass transfer and heat transfer inside the membrane module are schematically illustrated in Figure 4.

3.3. Flux and Recovery Determination. In the multichannel membrane condenser, mass transfer and heat transfer occur simultaneously (Figure 4). Membrane performance can be evaluated by water flux and recovery, and heat flux and recovery.

Water flux (J_w) and heat flux (q_w) across the membrane can be expressed respectively by

$$J_w = \frac{\Delta W}{\Delta t A} \tag{6}$$

$$q_w = \frac{C\dot{m}_l \Delta T + \dot{m}_T h(T)}{A} \tag{7}$$

where ΔW is the weight change (kg) of the liquid water during a period of Δt (h), A is the effective membrane area (m^2), C is the specific heat capacity of water (kJ·kg^{-1} K^{-1}), $\dot{m}_l$ is the liquid coolant (water) flow rate (kg·h^{-1}), and ΔT is the temperature change of the liquid water (K). $\dot{m}_T$ is the water transfer rate (kg·h^{-1}); $h(T)$ is the specific evaporation enthalpy of water at temperature T. Thus, the unit of mass flux is kg·m^{-2} h^{-1} and the unit of heat flux is kJ·m^{-2} h^{-1}.

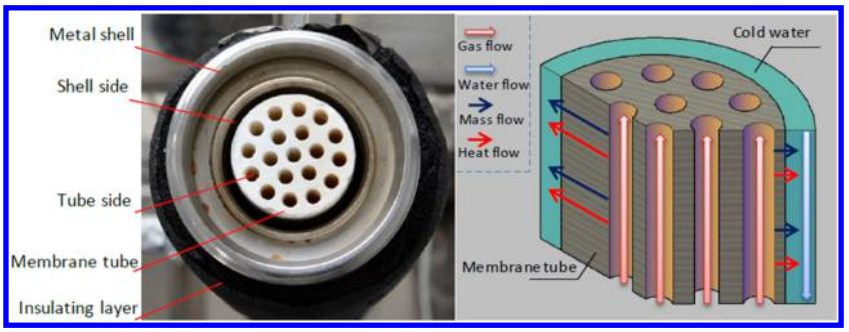

Figure 4. Cross section of the membrane module (left) and schematic diagram of mass and heat transfer (right) across the tubular membrane.

DOI: 10.1021/acs.iecr.6b00242
Ind. Eng. Chem. Res. XXXX, XXX, XXX−XXX

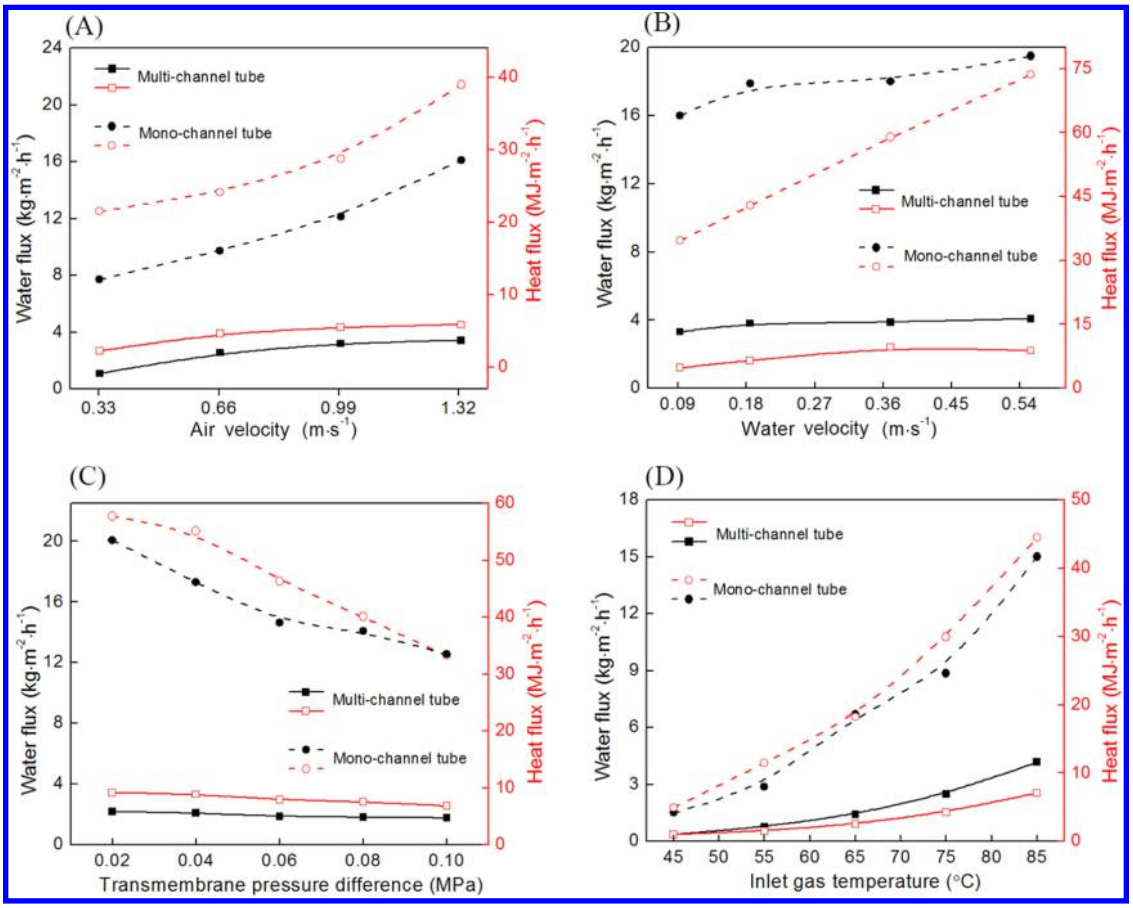

Figure 5. Water and heat fluxes as functions of (A) air velocity, (B) water velocity, (C) transmembrane pressure difference, and (D) inlet gas temperature. Typical experimental conditions: inlet gas temperature 75.5 °C, air flow rate 13 L·min^{-1}, water flow rate 5 L·h^{-1}, gas side gauge pressure 0.04 MPa, and liquid side gauge pressure 0 MPa.

Water recovery (γ) in the membrane condenser can be described as

$$\gamma\ (\%) = \frac{\Delta W}{W_{\text{vapor}}} \times 100 \tag{8}$$

where W_{vapor} is the weight of water vapor in the gaseous stream to the membrane module. W_{vapor} can be obtained by

$$W_{\text{vapor}} = \rho v r_{\text{mix}} \tag{9}$$

where ρ and v are the density (kg·m^{-3}) and volumetric flow rate (m^3·h^{-1}) of the air at a standard condition before the steam generator, and r_{mix} is the humidity percentage content of wetted air.

Heat recovery (η) in the membrane condensation system can be determined by

$$\eta\ (\%) = \frac{U_{\text{obtain}}}{U_{\text{inlet}}} \times 100 = \frac{q_w A}{h\dot{m}_{\text{inlet}}} \times 100 \tag{10}$$

where U_{obtain} is the obtained heat transfer rate (kJ·h^{-1}) across the membrane, U_{inlet} is the heat flow rate (kJ·h^{-1}) of the inlet gas stream to the membrane module, h is the specific enthalpy (kJ·kg^{-1}) of the gas stream, and $\dot{m}_{\text{inlet}}$ is the gas stream flow rate (kg·h^{-1}). Both h and $\dot{m}_{\text{inlet}}$ can be obtained with the help of the Humidity Calculator software (version 5.0) from Vaisala, Finland.

4. RESULTS AND DISCUSSION

4.1. Effect of Operational Parameters on Water and Heat Flux. Figure 5 shows the effects of experimental conditions including air velocity, water velocity, transmembrane pressure difference, and inlet gas temperature on water and heat fluxes. As the fluid (air or water) velocity increases, water and heat fluxes increase significantly for the monochannel membrane but slightly for the multichannel membrane (Figure 5A,B), indicating a significant boundary layer effect for the monochannel membrane but an insignificant boundary layer effect for the multichannel ceramic membrane. Water and heat fluxes decrease with the rise in transmembrane pressure difference due to the increased transfer resistance and reduced water and heat content in the gas stream (Figure 5C).[10] Mass and heat transfer rates of the ceramic tubular membranes increase exponentially with the rise in inlet gas temperature (Figure 5D), which is in agreement with the correlation between water vapor partial pressure and temperature in membrane distillation.[18,25] This suggests temperature-dependent water vapor partial pressure also plays an important role in mass and heat transfer in membrane condensation.

Compared with the monochannel ceramic tube, the multichannel ceramic tube exhibits much lower water and heat fluxes. This phenomenon is most likely caused by the difference in mass and heat transfer resistances between the multichannel and monochannel membranes. In the multichannel ceramic tube water and heat need to pass a relatively long distance from the hot gas side to the cold water side

DOI: 10.1021/acs.iecr.6b00242
Ind. Eng. Chem. Res. XXXX, XXX, XXX−XXX

(Figures 4 and 6). Namely, multichannel ceramic tubes have larger mass and heat transfer resistances than monochannel

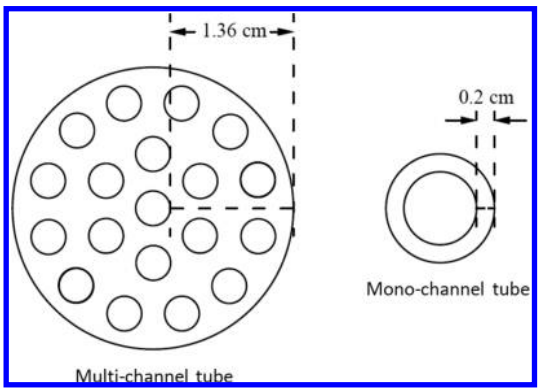

Figure 6. Cross sections of multichannel and monochannel tubes.

ones. The results indicate that monochannel tubular membranes outperform multichannel membranes in terms of mass and heat transfer rates.

Comparison of overall heat transfer coefficients between the multichannel ceramic membrane and the monochannel ceramic membrane is described in Table 2. The facile heat transfer

Table 2. Comparison of Overall Heat Transfer Coefficients ($W \cdot m^{-2} \cdot K^{-1}$) between the Multichannel Tubular Membrane and the Monochannel Tubular Membrane

	overall heat transfer coefficient ($W \cdot m^{-2} \cdot K^{-1}$)	
air flow velocity ($m \cdot s^{-1}$)	multichannel tube	monochannel tube
0.332	42.7	246.8
0.664	98.9	252.8
0.996	99.4	311.7
1.328	102.9	364.3

coefficient of the monochannel ceramic membrane is much higher than that of the multichannel one. For example, the heat transfer coefficient of the monochannel membrane is up to 312 $W \cdot m^{-2} \cdot K^{-1}$, which is around 3 times higher than that of the multichannel membrane (99 $W \cdot m^{-2} \cdot K^{-1}$) when the gas velocity is 0.996 $m \cdot s^{-1}$. Nevertheless, the overall heat transfer coefficient of the multichannel membrane at a low gas velocity is still comparable with that of a conventional heat exchanger in flue gas heat recovery.[26] Under optimized operational conditions with high fluid velocities, multichannel membranes can be superior to conventional heat exchangers in heat recovery because both conductive and convective heat transfer results in membrane condensation.

Mass and heat transfer performance of the multichannel membrane displays trends similar to that of the monochannel membrane: mass and heat transfer rates increase with the rise in gas velocity, water velocity, and inlet gas temperature, but decrease with the rise in transmembrane pressure difference (Figure 5 and Table 2). Relevant explanations have been detailed in our previous study.[10] However, it is more obvious that operational parameters (i.e., fluid velocity, transmembrane pressure difference, and inlet gas temperature) have less effects on mass and heat transfer rates of the multichannel ceramic membrane compared with the monochannel membrane. In our investigations, laminar flow occurs in the flow velocity range (Reynolds number < 400). Operational parameters are anticipated to have significant influences on the mass and heat transfer rates due to the boundary layer effect. However, this general rule does not apply to the transport performance of the multichannel membrane. This phenomenon implies that membrane resistance rather than boundary layer resistance dominates the mass and heat transfer when a multichannel membrane is used for water and heat recovery. Therefore, physical characteristics of multichannel tubular membranes (e.g., thickness of channel wall, pore size, and porosity) should be further optimized to minimize membrane resistance before these membranes can be employed for water and heat recovery via condensation.

In membrane condensation, the mass transfer mechanism is thought to be very complicated. Multilayer diffusion and capillary condensation may dominate mass transfer in this process,[4,20,21,27] and the condensed water vapor transport through the membrane via a pseudoliquid phase transport.[20] Systematic investigation of the mass transfer mechanism in membrane condensation for water and heat recovery is needed in the future.

4.2. Effect of Operational Parameters on Water and Heat Recovery. Figure 7 shows the effects of operational parameters on water and heat recoveries in membrane condensation. The multichannel tubular membrane exhibits water recoveries comparable with those of the monochannel membrane under the same experimental conditions, although the water transfer rate of the former is much lower than that of the latter. However, heat recoveries of the multichannel membrane are obviously lower than those of the monochannel membrane. It could be attributed to the lower water transfer rate of the multichannel membrane. Also, the wall of each channel is so thick in the multichannel tube (i.e., very long heat transfer distance) that thermal conductive heat transfer is very low, and even can be ignored compared with advective heat transfer.

Water and heat recoveries of the monochannel membrane are not proportional, while those of the multichannel membrane are almost proportional. This interesting phenomenon can be explained by mass and heat transfer differences between the monochannel membrane and the multichannel membrane. In the monochannel membrane, heat transfer is determined by the overall thermal conductivity (including those of the boundary layer and membrane) and convective heat flow (which is proportional to mass transfer), leading to a disproportional correlation between heat recovery and water recovery.[10] In the multichannel membrane, thermal conductive heat flow across the boundary layer and membrane is negligible due to the very thick wall of the channels (Figure 6), and heat transfer is governed by convective heat transfer (which is proportional to mass transfer). As a result, water and heat recoveries show a proportional correlation in membrane condensation with the multichannel tubular membrane.

In Figure 7A–C, the multichannel membrane displays changes in water and heat recoveries similar to those of the monochannel membrane under different gas velocities, water velocities, and transmembrane pressure difference. Related discussion and explanations can be found in our previous work.[10] However, water and heat recoveries of the multichannel membrane decline with the rise in inlet gas temperature. In fact, inlet gas contains a higher content of water vapor and enthalpy (heat) at higher temperatures; if the membrane cannot effectively recover the water and heat to the liquid water side,

DOI: 10.1021/acs.iecr.6b00242
Ind. Eng. Chem. Res. XXXX, XXX, XXX−XXX

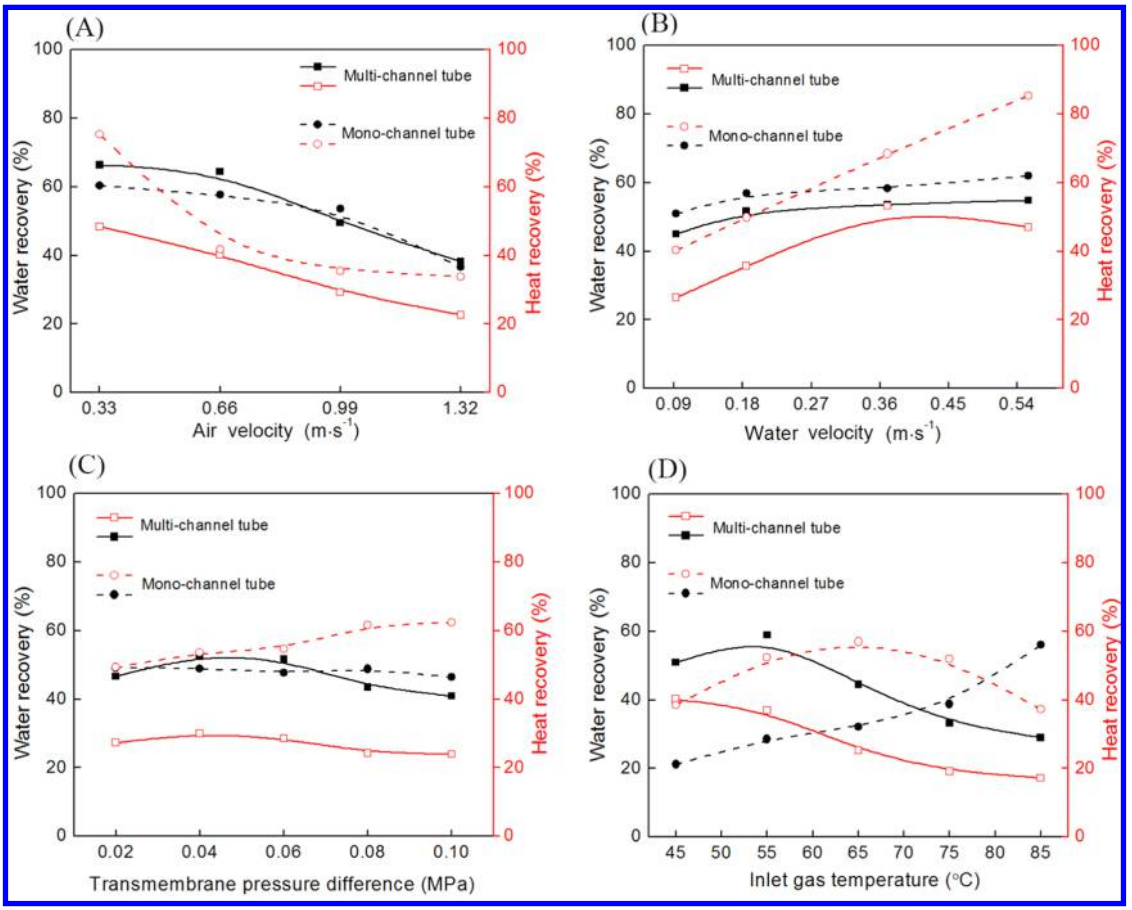

Figure 7. Water and heat recoveries as functions of (A) air velocity, (B) water velocity, (C) transmembrane pressure difference, and (D) inlet gas temperature. Typical experimental conditions: inlet gas temperature 75.5 °C, air flow rate 13 L·min^{-1}, water flow rate 5 L·h^{-1}, gas side gauge pressure 0.04 MPa, and liquid side gauge pressure 0 MPa.

outlet gas will still have high water vapor and enthalpy, resulting in lower water and heat recoveries (Figure 7D).

4.3. Multichannel Membrane vs Monochannel Membrane. Previously, we used a monochannel tubular membrane with an inner diameter of 0.008 m for water and heat recovery from gas streams. In the current study, we selected a 19-channel tubular membrane and the inner diameter of each channel is 0.0038 m. The multichannel tube has a higher effective membrane area per volume than the monochannel tube (Figure 8A). Compared with the monochannel membrane, however, to treat a certain volume of gas streams, much more membrane area will be required for the multichannel membrane (Figure 8B) mainly due its much lower water and heat fluxes (Figure 5). Figure 8C compares the tube length for the two types of membranes required to treat a certain volume of waste gas. The required monochannel tube is much longer than the multichannel tube. Unfortunately, monochannel tubes become fragile in extended length. This is one of the reasons that monochannel tubes are generally bundled in practical applications.[4,11]

Cross sections of the multichannel and monochannel tubes are also compared (Figure 6). The 19-channel tube has three types of channels: one central channel, six intermediate channels, and 12 peripheral channels. Transport distances from the three types of channels to the outer phase are different. For example, in the multichannel tube the transfer distance from the central channel to the outer phase is 0.0136 m, almost 7 times longer than the distance in the monochannel tube. The estimated heat transfer resistance in the multichannel tube is about 5 times larger than that in the monochannel tube based on eq 2. As a result, mass and heat transfer rates in the multichannel tubular membrane are much lower compared with the monochannel membrane. However, the multichannel membrane has much higher volumetric mass and heat transfer coefficients (5−11 and 7−15 times higher in mass and heat, respectively) than the monochannel tubular membrane (Figure 8D). This pronounced advantage of the multichannel membrane makes it promising in practical large-scale applications.

From the above discussion, multichannel tubular membranes have lower mass and heat transfer rates, and lower heat recoveries, than monochannel tubular membranes mainly due to the longer transport distance (larger resistance). Although the required monochannel membrane may be longer and thus more fragile, these disadvantages can be overcome by bundling (Figure 1A). Multichannel membranes are very promising in practical water and heat recovery applications due to their much higher volumetric mass and heat transfer coefficients compared with monochannel membranes. In addition, mass and heat transfer performance of multichannel membranes can be improved by optimizing the membrane properties (e.g., reducing the thickness of the channel wall, changing the channel number, and increasing membrane porosity).[14] Related work will be carried out in our future investigations.

In practical heat and water recovery from huge volumes of gas streams, employing bundled monochannel tubular mem-

DOI: 10.1021/acs.iecr.6b00242
Ind. Eng. Chem. Res. XXXX, XXX, XXX−XXX

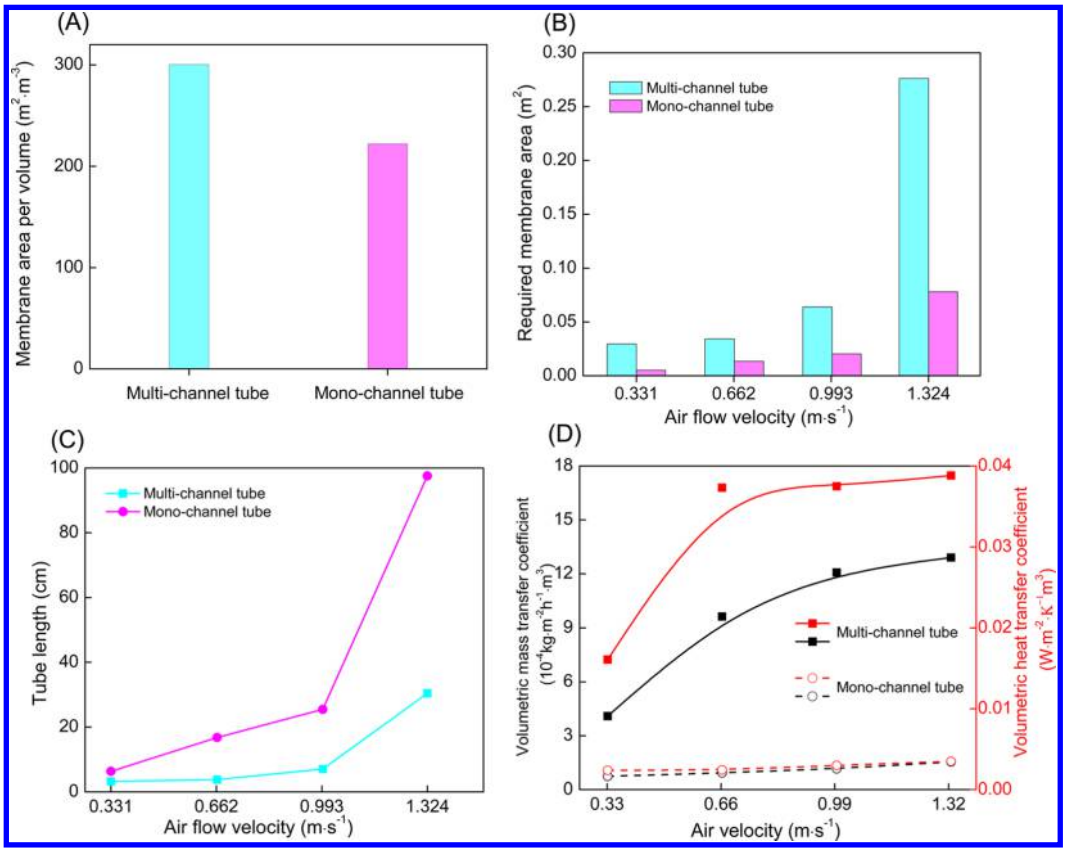

Figure 8. Theoretical and experimental comparison of multichannel tube and monochannel tube in terms of (A) membrane area per volume, (B) required membrane area, (C) tube length, and (D) volumetric mass transfer coefficient. Simulated experimental conditions: relative gas humidity 100%, gas mixture temperature 75 °C, liquid flow rate 5 $L \cdot h^{-1}$, liquid side gauge pressure 0 MPa, and gas side gauge pressure 0.04 MPa.

branes is a reasonable option due to the high interfacial membrane areas and high mass and heat transfer rates. However, the costs from manufacturing, potting, and sealing of monochannel membranes are theoretically higher than those of multichannel tubular membranes because the latter membranes are once-molded and the modules are much simpler. Additionally, once-molded tubular membranes with self-organized microchannels are anticipated to have higher interfacial membrane areas and mechanical strength than bundled monochannel tubes, which can compensate the high transfer resistance in practical applications.

5. CONCLUSIONS

To the best of our knowledge, for the first time we report a multichannel ceramic tubular membrane for water and heat recovery from gas streams. Mass and heat transfer performances of the multichannel tubular membrane are investigated and compared with those of a monochannel tubular membrane. Some important and new findings are the following:

(i) Compared with the monochannel tubular membrane, the multichannel membrane has much larger mass and heat transfer resistances, leading to lower mass and heat transfer rates.

(ii) Operational parameters have less effects on mass and heat transfer in the multichannel membrane, suggesting that transfer resistance from the membrane itself rather than the boundary layers dominates mass and heat transfer in membrane condensation using multichannel membranes.

(iii) The multichannel membrane shows larger volumetric mass and heat transfer coefficients, comparable water recoveries, but lower heat recoveries compared with the monochannel tubular membrane.

(iv) Water and heat recoveries show a proportional correlation in membrane condensation with the multichannel tubular membrane, indicating that heat transfer is governed by the convective heat transfer and thermal conductive heat transfer is negligible in the multichannel membrane.

AUTHOR INFORMATION

Corresponding Authors

*Tel.: +61-2-4960-6127. E-mail: shuaifei.zhao@mymail.unisa.edu.au.

*Tel.: +86-25-83172279. E-mail: hqi@njtech.edu.cn.

Notes

The authors declare no competing financial interest.

ACKNOWLEDGMENTS

This work is supported by the National Natural Science Foundation of China (21276123, 21490581), the National High Technology Research and Development Program of China (2012AA03A606), and the "Summit of the Six Top Talents" Program of Jiangsu Province. Special thanks have to go to Prof. Damian Gore for his significant help with the revision of this paper.

REFERENCES

(1) Shannon, M. A.; Bohn, P. W.; Elimelech, M.; Georgiadis, J. G.; Marinas, B. J.; Mayes, A. M. Science and technology for water purification in the coming decades. *Nature* **2008**, *452*, 301−310.

DOI: 10.1021/acs.iecr.6b00242
Ind. Eng. Chem. Res. XXXX, XXX, XXX−XXX

(2) Du, K.; Lin, B. Understanding the rapid growth of China's energy consumption: A comprehensive decomposition framework. *Energy* **2015**, *90*, 570−577.
(3) Judd, S.; Jefferson, B. *Membranes for Industrial Wastewater Recovery and Re-use*; Elsevier: 2003.
(4) Wang, D.; Bao, A.; Kunc, W.; Liss, W. Coal power plant flue gas waste heat and water recovery. *Appl. Energy* **2012**, *91*, 341−348.
(5) Water Capture. http://www.watercapture.eu.
(6) Macedonio, F.; Brunetti, A.; Barbieri, G.; Drioli, E. Membrane Condenser as a New Technology for Water Recovery from Humidified "Waste" Gaseous Streams. *Ind. Eng. Chem. Res.* **2013**, *52*, 1160−1167.
(7) Brunetti, A.; Santoro, S.; Macedonio, F.; Figoli, A.; Drioli, E.; Barbieri, G. Waste Gaseous Streams: From Environmental Issue to Source of Water by Using Membrane Condensers. *Clean: Soil, Air, Water* **2014**, *42*, 1145−1153.
(8) Drioli, E.; Santoro, S.; Simone, S.; Barbieri, G.; Brunetti, A.; Macedonio, F.; Figoli, A. ECTFE membrane preparation for recovery of humidified gas streams using membrane condenser. *React. Funct. Polym.* **2014**, *79*, 1−7.
(9) Macedonio, F.; Cersosimo, M.; Brunetti, A.; Barbieri, G.; Drioli, E. Water recovery from humidified waste gas streams: Quality control using membrane condenser technology. *Chem. Eng. Process.* **2014**, *86*, 196−203.
(10) Wang, T.; Yue, M.; Qi, H.; Feron, P. H. M.; Zhao, S. Transport membrane condenser for water and heat recovery from gaseous streams: Performance evaluation. *J. Membr. Sci.* **2015**, *484*, 10−17.
(11) Bao, A.; Wang, D.; Lin, C.-X. Nanoporous membrane tube condensing heat transfer enhancement study. *Int. J. Heat Mass Transfer* **2015**, *84*, 456−462.
(12) Wang, D. *Advanced Energy and Water Recovery Technology from Low Grade Waste Heat*; Gas Technology Institute: 2011.
(13) Avila, P.; Montes, M.; Miró, E. E. Monolithic reactors for environmental applications: A review on preparation technologies. *Chem. Eng. J.* **2005**, *109*, 11−36.
(14) Lee, M.; Wu, Z.; Wang, B.; Li, K. Micro-structured alumina multi-channel capillary tubes and monoliths. *J. Membr. Sci.* **2015**, *489*, 64−72.
(15) Zhang, L.-Z. Progress on heat and moisture recovery with membranes: From fundamentals to engineering applications. *Energy Convers. Manage.* **2012**, *63*, 173−195.
(16) Che, D.; Da, Y.; Zhuang, Z. Heat and mass transfer characteristics of simulated high moisture flue gases. *Heat Mass Transfer* **2005**, *41*, 250−256.
(17) Yan, S.; Zhao, S.; Wardhaugh, L.; Feron, P. H. M. Innovative Use of Membrane Contactor as Condenser for Heat Recovery in Carbon Capture. *Environ. Sci. Technol.* **2015**, *49*, 2532−2540.
(18) Zhao, S.; Cao, C.; Wardhaugh, L.; Feron, P. H. M. Membrane evaporation of amine solution for energy saving in post-combustion carbon capture: Performance evaluation. *J. Membr. Sci.* **2015**, *473*, 274−282.
(19) Zhao, S.; Feron, P. H. M.; Cao, C.; Wardhaugh, L.; Yan, S.; Gray, S. Membrane evaporation of amine solution for energy saving in post-combustion carbon capture: Wetting and condensation. *Sep. Purif. Technol.* **2015**, *146*, 60−67.
(20) Uhlhorn, R. J. R.; Keizer, K.; Burggraaf, A. J. Gas transport and separation with ceramic membranes. Part I. Multilayer diffusion and capillary condensation. *J. Membr. Sci.* **1992**, *66*, 259−269.
(21) Horikawa, T.; Do, D. D.; Nicholson, D. Capillary condensation of adsorbates in porous materials. *Adv. Colloid Interface Sci.* **2011**, *169*, 40−58.
(22) Choi, J.-G.; Do, D. D.; Do, H. D. Surface Diffusion of Adsorbed Molecules in Porous Media: Monolayer, Multilayer, and Capillary Condensation Regimes. *Ind. Eng. Chem. Res.* **2001**, *40*, 4005−4031.
(23) Phattaranawik, J.; Jiraratananon, R.; Fane, A. G. Effect of pore size distribution and air flux on mass transport in direct contact membrane distillation. *J. Membr. Sci.* **2003**, *215*, 75−85.
(24) Qi, H.; Niu, S.; Jiang, X.; Xu, N. Enhanced performance of a macroporous ceramic support for nanofiltration by using α-Al2O3 with narrow size distribution. *Ceram. Int.* **2013**, *39*, 2463−2471.
(25) Zhao, S.; Feron, P. H. M.; Xie, Z.; Zhang, J.; Hoang, M. Condensation studies in membrane evaporation and sweeping gas membrane distillation. *J. Membr. Sci.* **2014**, *462*, 9−16.
(26) Shi, X.; Che, D.; Agnew, B.; Gao, J. An investigation of the performance of compact heat exchanger for latent heat recovery from exhaust flue gases. *Int. J. Heat Mass Transfer* **2011**, *54*, 606−615.
(27) Qiao, S. Z.; Bhatia, S. K.; Zhao, X. S. Prediction of multilayer adsorption and capillary condensation phenomena in cylindrical mesopores. *Microporous Mesoporous Mater.* **2003**, *65*, 287−298.

DOI: 10.1021/acs.iecr.6b00242
Ind. Eng. Chem. Res. XXXX, XXX, XXX−XXX